



Characterization of copper SERS-active substrates prepared by electrochemical deposition

Jitka Cejkova^{a,*}, Vadym Prokopec^b, Sona Brazdova^b, Alzbeta Kokaislova^b, Pavel Matejka^b, Frantisek Stepanek^a

^a Institute of Chemical Technology Prague, Department of Chemical Engineering, Technicka 5, 166 28 Prague 6, Czech Republic

^b Institute of Chemical Technology Prague, Department of Analytical Chemistry, Technicka 5, 166 28 Prague 6, Czech Republic

ARTICLE INFO

Article history:

Received 16 January 2009

Received in revised form 8 April 2009

Accepted 8 April 2009

Available online 3 May 2009

Keywords:

Surface Enhanced Raman Scattering (SERS)

Atomic Force Microscopy (AFM)

Scanning Electron Microscopy (SEM)

Copper

Electrochemical deposition

ABSTRACT

Surface Enhanced Raman Scattering (SERS) on copper substrates of various morphologies, prepared by electrochemical deposition on platinum targets, was investigated. The substrate preparation procedures differed by the coating bath compositions, applied current densities and the duration of individual steps. The surface morphology of the substrates was visualized by means of Atomic Force Microscopy (AFM) and Scanning Electron Microscopy (SEM). SERS spectra of selected organic thiols were measured and the relation between SERS spectral intensity and the surface structure of SERS-active substrates was studied. It has been shown that good Raman surface enhancement can be achieved on the copper substrates prepared by electrochemical deposition from ammoniac baths. Copper substrates fabricated from acidic baths did not show efficient Raman surface enhancement. The results of microscopic measurements demonstrated that the average surface roughness value does not play a substantial role, whereas the shape of the surface nanostructures is a key parameter.

© 2009 Elsevier B.V. All rights reserved.

1. Introduction

Surface Enhanced Raman Scattering (SERS) spectroscopy is a powerful analytical technique usually providing a Raman signal enhancement of the order of 10^6 . The enhancement factor can be up to 10^{14} [1], which allows the technique to be sensitive enough to detect even single molecules. SERS is based on the inelastic photon scattering of molecules positioned in the proximity of a nanostructured metal surface. This method is widely applied to study a variety of analytes in electrochemistry, surface science, material science, nanotechnology and biochemistry [2].

The exact nature of the SERS enhancement of Raman signals is not fully understood but appears to be caused by two contributing mechanisms of enhancement, namely the long-range electromagnetic effect and short-range chemical effect [3]. (i) The electromagnetic enhancement is a consequence of the interaction of the incident electric field (from the incident radiation) with electrons in the metal surface. It leads to excitation of surface plasmons, thereby enhancing the electric field at the metal surface. This enhancement is dominant and it is a direct consequence of the roughened nanostructure on a metal surface. These roughened features can be created in a number of ways; for example

oxidation–reduction cycles (ORC) on electrode surfaces [4], deposition of metal microspheres or nanoparticles onto a substrate [5], corrosive etching or electrochemical roughening [6], ablation of metal foils by laser pulses [7] or electron beam lithography [8]. All of the methods mentioned above leave the substrate surface covered with small metal particles or aggregates of particles responsible for the Raman enhancement [3,9]. (ii) The chemical enhancement is caused by the formation of a charge-transfer complex between the metal surface and the analyte molecule. The chemical mechanism usually gives a lesser contribution (up to 10^2) to the overall SERS effect [9].

Theoretically, SERS phenomena can occur on all roughened metal substrates, but the efficiency of Raman enhancement depends on the nature of the nanostructured metal material with respect to the excitation wavelength used. There is a resonance condition between the frequency of incident radiation and the excitation wave on the metal surface, which relates to the dielectric function of the individual metal. Generally, metals with high optical reflectivity, such as silver, gold or copper meet this condition and are able to give efficient SERS effect in visible and/or near-infrared range. Since the discovery of the SERS phenomenon in the 1970s, SERS spectra of molecules adsorbed on gold or silver substrates have been extensively studied. On the contrary, copper as a SERS-active substrate has been used rarely, owing to its chemical instability as well as relatively weaker SERS activity [10]. Nevertheless, copper is a very promising material from the point of

* Corresponding author. Tel.: +420 220 443 833; fax: +420 220 444 320.
E-mail address: jitka.cejkova@vscht.cz (J. Cejkova).

view of chemisorption of various types of organic compounds and the comparatively low costs for substrate preparation in routine analysis. Other transition metals such as Fe, Pt, Ni or Co with low optical reflectivity are regarded as non-SERS-active metals, although some groups have shown the possibility to utilize these metals for obtaining relatively weakly enhanced SERS signals as well [11–13].

An essential parameter influencing the resulting enhancement is the morphology of the substrate surface. Several techniques can be used for the characterization of surface structures, such as Atomic Force Microscopy (AFM) [14], Scanning Tunneling Microscopy (STM), Scanning Electron Microscopy (SEM), or Transmission Electron Microscopy (TEM). The main advantage of using AFM is to characterize surface structures so that it provides a true 3D surface profile and enables quantitative measurements of nanoscale roughness. A disadvantage of AFM is the relatively limited scanner range, which is typically of the order of $100 \times 100 \mu\text{m}$. If information about surface uniformity on a larger length-scale is required, several different areas of the sample have to be scanned separately. The z-range of AFM (typically $5 \mu\text{m}$) is a limitation that prevents the measurements of very rough samples. SEM makes it possible to obtain images at different length-scales, but the disadvantage of standard SEM is the unavailability of quantitative surface roughness evaluation.

In our recent works [15,16], we have studied gold and silver SERS-active substrates fabricated using procedures consisting of electrochemical deposition of metal layers and further roughening with ORC treatment. The nanostructures of the metal surfaces were characterized by means of AFM. The relation between Raman enhancement and surface morphology was found and described. In the present paper, we have focused especially on copper SERS-active substrates prepared by electrochemical deposition. The bath composition, the number of current steps and the levels of current used during the metal coating process were systematically varied. The main reason for this was to understand how the bath composition and the increasing applied current influenced the nanostructure of the prepared surface, which was consequently determined by AFM and SEM measurements.

4-Aminobenzenethiol (4-ABT) and 16-mercaptohexadecanoic acid (16-MDHA) were chosen as analytes for our SERS measurements because these molecules adsorb very favorably on copper by forming a Cu-thiolate bond. Previous studies with the above analytes on copper include the work of Shin et al. [17] who investigated the conversion of 4-nitrobenzenethiol to 4-ABT on Cu foil etched using dilute HNO_3 solution by means of SERS. Kim et al. [18] studied the effect of Ag and Au nanoparticles on the SERS of 4-ABT assembled on powdered Cu. Bozzini et al. [19] studied

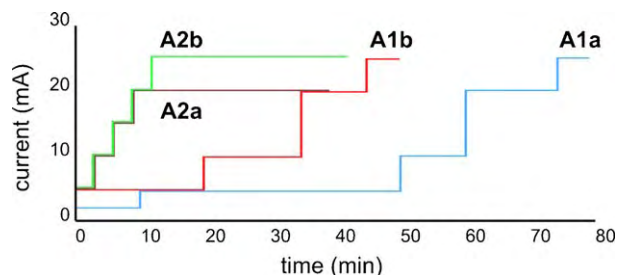


Fig. 1. Conditions of copper SERS-active surfaces preparation from an acidic bath.

electrodeposition of Cu from acidic sulphate solution, but all Raman measurements were carried out in situ in the electrochemical cell. In the present paper, we studied Raman enhancement in dependence on surface morphology of SERS-active copper substrate. The relation of SERS efficiency and the surface structure of the substrates are described.

2. Experimental

2.1. SERS-active surfaces fabrication

All experiments were performed on massive platinum targets (diameter 10 mm, thickness 2 mm, Safina, Czech Republic), which were coated by a copper layer using electrochemical procedures. The platinum targets were first polished with metallographic paper (Emery Paper, SIA, Switzerland), alumina and calcium carbonate in order to obtain a clean macroscopically smooth surface. The polished targets were then immersed into the “piranha solution” (a 1:3 v/v mixture of 30% hydrogen peroxide and 98% sulfuric acid) for 30 min and finally thoroughly washed with redistilled water. After the pretreatment of platinum targets, the electrochemical procedure of copper deposition followed. All procedures were performed in an electrochemical cell where a flat copper electrode was used as the anode and the platinum target as the cathode. The primary tests of various composition of the electrochemical bath were aimed at fabricating “spectroscopically pure” surfaces (there should be no detectable interferences in the spectra of the surface of SERS-active substrate prior to the deposition of a compound studied). Considering the results of preliminary experiments, copper coating was performed either from an acidic or an ammoniac bath. The acidic bath consisted of a saturated CuSO_4 solution in distilled water acidified by concentrated H_2SO_4 (98%). The ammoniac baths contained complexations of $[\text{Cu}(\text{NH}_3)_4]^{2+}$. It was prepared by the addition of NaOH

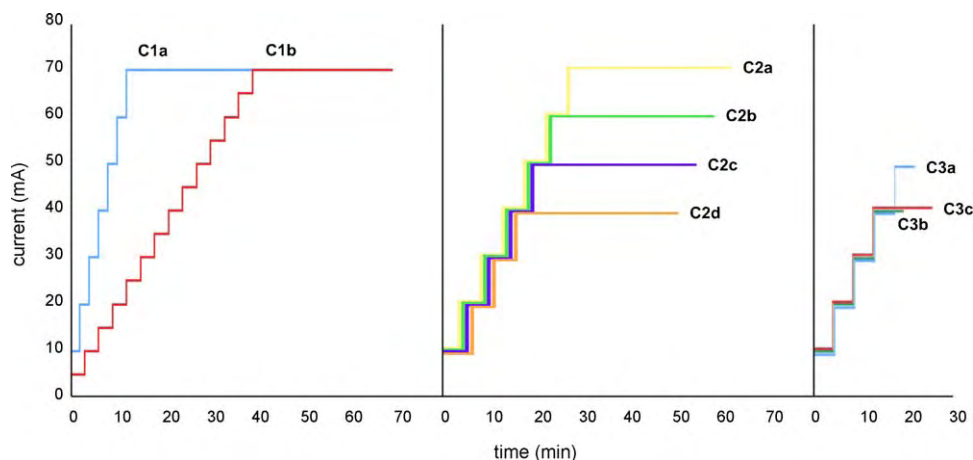


Fig. 2. Conditions of copper SERS-active surfaces preparation from an ammoniac bath.

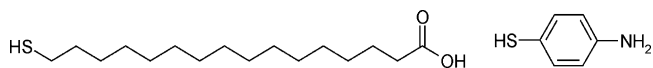


Fig. 3. Structural formulas of the analyte molecules: 16-mercaptohexadecanoic acid (16-MHDA) and 4-aminobenzenethiol (4-ABT).

solution into a saturated solution of CuSO_4 or $\text{Cu}(\text{NO}_3)_2$ and the formed precipitate was dissolved in a NH_3 solution (25% w/v). Different preparation steps with various current values (from 2 mA up to 70 mA) and duration were tested during all coating processes. The preparation conditions are summarized in Figs. 1 and 2.

2.2. Deposition of organic substances

4-ABT (Fluka) and 16-MHDA (Sigma) (Fig. 3) were used during this study for the evaluation of SERS activity of copper substrates. All deposition processes were performed from solutions of 4-ABT (1 mg 4-ABT in 4 ml methanol p.a.) or 16-MHDA (1.7 mg in 4 ml methanol p.a.). The individually fabricated SERS-active substrate was immersed into the sample solution for 24 h. Afterwards the target was taken out of the solution and in some cases it was rinsed with solvent repeatedly, in order to remove all excessive thiols that were not fixed (by either covalent or noncovalent interactions) onto the surface.

2.3. Raman measurements

Near-infrared excited reference FT-Raman spectra of the samples were collected on a FT-Raman spectrometer Bruker [FT-NIR spectrometer EQUINOX 55, Raman module FRA 106/S, Nd:YAG laser (excitation line 1064 nm) and Ge diode detector cooled with liquid nitrogen] (Bruker Optics). A standard 4 cm^{-1} spectral resolution, 1024 scans, 'zero filling' eight and Blackmann-Harris cosine apodization function was used for all data accumulation and Fourier-transform processing. The FT-Raman spectrometer was equipped with a thin layer chromatographic (TLC) mapping stage (Bruker Optics) designed by the manufacturer for macroscopic mapping of TLC plates.

SERS spectra with visible excitation were collected using a disperse Raman spectrometer LabRam (Dilor Jobin-Yvon), which was equipped with microscopic objectives (magnification from $10\times$ to $100\times$) and a computer-controlled mapping sample stage. The source of excitation radiation was either an external Argon-ion laser (488 nm, Melles Griot) with adjustable laser power up to 30 mW or an internal laser (633 nm, He-Ne, 25 mW). A thermoelectrically cooled charge-coupled device (CCD 1024×256 pixels) operating at approximately -60°C was used as the detector with $2\text{--}4 \text{ cm}^{-1}$ resolution. All spectra were referenced with respect to a silicon wafer band at 521 cm^{-1} .

2.4. Atomic force microscopy and scanning electron microscopy

The surface structure of copper-coated targets was imaged by an Atomic Force Microscope (AFM) Ntegra (NT-MDT) in the semi-contact mode. Silicon high accuracy tips HA_NC (NT-MDT) with typical resonant frequency of 120 kHz, force constant of 3.4 N/m, curvature radius of 10 nm and a tip aspect ratio 5:1 were used. Scanning by sample configuration was selected. The scanner with a maximum range of $100 \times 100 \mu\text{m}$ was chosen. All measurements were carried out in air at room temperature. After scanning, the images were flattened and the roughness was evaluated using Nova software (NT-MDT). SEM images were obtained with a JCM-5700 CarryScope (JEOL) Scanning Electron Microscope (SEM).

2.5. Roughness evaluation of the copper surfaces

The most common parameters used for roughness evaluation are the average roughness (R_a) and root-mean-square roughness (R_q). R_a is the arithmetic average of the absolute values of the roughness profile ordinates and R_q is the root mean square average of the roughness profile ordinates. Because R_q is more sensitive to peaks and valleys than R_a , in this work the surface morphology of the copper samples was quantitatively described by the R_q parameter, provided by the AFM software Nova (NT-MDT). The roughness was evaluated on areas of $50 \times 50 \mu\text{m}$.

3. Results and discussion

3.1. Morphological characterization of the copper surfaces

All preparation procedures of copper SERS-active substrates described in this paper were aimed at the formation of macroscopically uniform surfaces (comparable with the size of the target) and the achievement of uniform enhancement of Raman signal of the compounds adsorbed onto the surface. As stated in the Introduction, one of the main factors affecting the enhancement is the substrate morphology on the nanoscale level. The nanostructure of the surface can be modified with the change of applied current value and duration of current steps during the metal coating process.

Each preparation procedure started with steps of low current values in order to form a homogeneous continuous copper layer on a bare platinum target, which should cover all imperfections on the underlying Pt surface that may have been caused by pretreatment procedures. After the formation of this bright copper film, higher current was applied in order to form rougher copper nanostructures on the surface. It was necessary to optimize the duration of these two main parts of the preparation procedure, as detailed below.

3.1.1. Copper substrates prepared from an acidic bath

Preparation procedures from acidic baths A1 and A2 are summarized in Fig. 1. In procedure A1 the conditions of low current steps were applied for at least 30 min (steps 1–3 in A1a and 1–2 in A1b) in order to form a thick bright copper layer. Afterwards higher

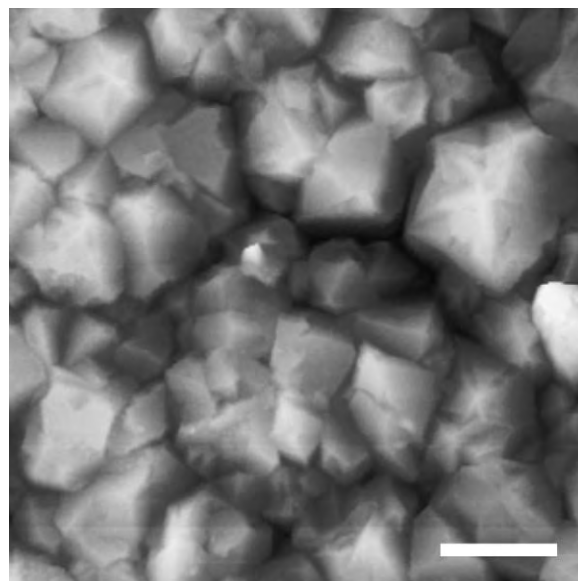


Fig. 4. AFM image of copper SERS-active substrate prepared according to procedure A1b. The scale bar represents $10 \mu\text{m}$.

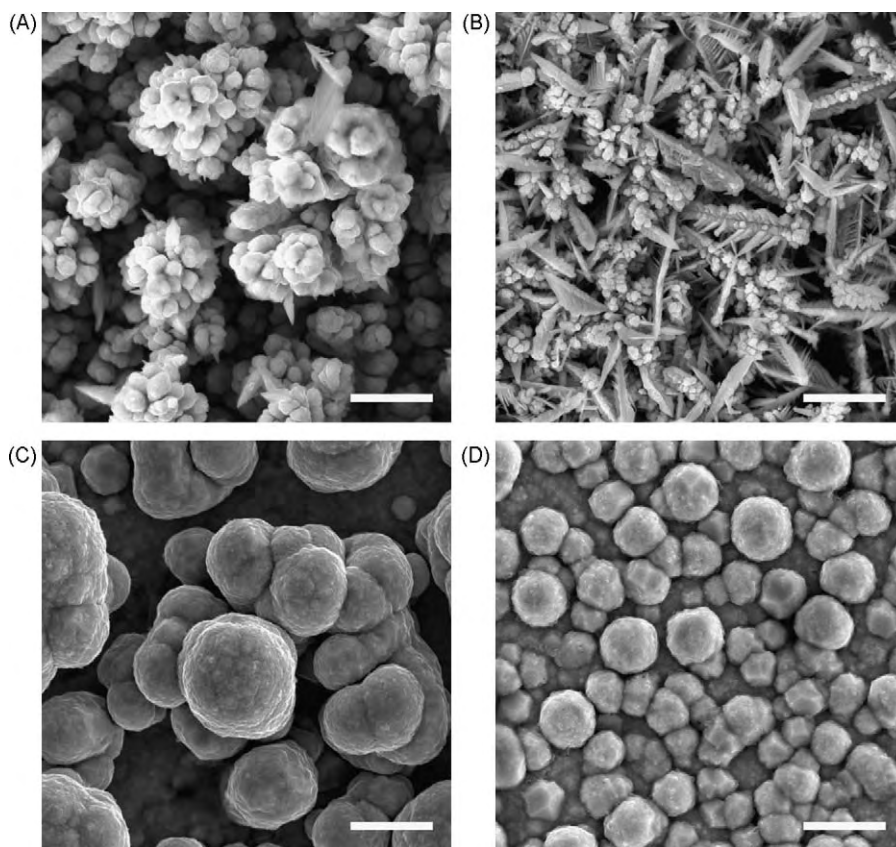


Fig. 5. SEM images of copper SERS-active substrates prepared according to procedures (A) C1b, (B) C2b, (C) C3b and (D) C3c. The scale bar represents 10 μm .

current was applied with shorter duration of individual steps. An AFM image of copper SERS-active substrate prepared according to procedure A1b is shown in Fig. 4. Qualitatively, all copper surfaces prepared from an acidic bath appeared similar: copper formed crystal-like structures with characteristic dimensions in the range of 0.5–20 μm . Their distribution on the surface was uniform even at a larger length-scale. Somewhat larger copper particles (10–20 μm) appeared on copper substrates prepared according to the procedure A1b, whereas procedure A1a gave rise to smaller crystallites in the size range of 2–8 μm . The surface roughness of the copper samples was quantitatively described through the root-mean-square roughness (R_q) parameter, determined by AFM. R_q of copper substrate A1a was 432 ± 32 nm and that of A1b substrate was 805 ± 60 nm.

In order to vary the surface features and consequently the surface enhancement factor, the preparation procedures were modified by changing the duration of the individual steps (procedures A2a and A2b in Fig. 1). The first part of each procedure was shortened and the last step with the highest current value was prolonged several times. Nevertheless, surface topography of A2a and A2b substrates did not differ dramatically from substrates prepared according to procedures A1a and A1b, i.e. the surface was mainly covered by crystallites with a morphology shown in Fig. 4. Besides that, a small proportion of irregularly shaped particles in the size range of 0.5–10 μm also appeared on the substrate. The R_q parameters of surfaces prepared according to procedures A2a and A2b were 312 ± 13 nm and 255 ± 7 nm, respectively. It is evident from these values that the modification of the preparation procedures from A1 to A2 causes a reduction of the surface roughness.

3.1.2. Copper substrates prepared from an ammoniac bath

Substrate preparation from new ammoniac baths for metal coating was tested next. The applied current as function of time

during preparation procedures C1–C3 is summarized in Fig. 2. During copper coating using the ammoniac bath, the primary bright copper film began to form at higher currents than in the case of the acid bath. In light of this, a larger number of current steps in periodic sequences was used, with the last step always being the longest.

The preparation of substrates from ammoniac baths resulted in the formation of qualitatively different nanoscale surface structures compared with those prepared from acidic baths. No regular crystal-like features appeared on the surface. Instead, a Cu layer was formed from structures of various complex shapes specific to the preparation conditions (cf Fig. 5). Due to the very complex surface structures that included concave as well as convex features, it was not possible to use AFM for measurements and roughness evaluation.

Preparation method C1 involved gradually increasing the applied current for short time intervals (2 min for method C1a and 3 min for method C1b). The last step was the application of 70 mA current for half an hour. This course of preparation led to the formation of cauliflower-like structures on the substrate surfaces. A SEM image of copper substrate prepared according to procedure C1b is shown in Fig. 5A.

Preparation methods C2 were derived from C1; there was a difference in the duration of the last high current applications, which lasted only 15 min in methods C2. The highest current applied was decreasing from 70 mA to 40 mA in preparation procedures C2a–C2d. Surfaces obtained using methods C2 consisted of fractured nanoaggregates with barb-like structure (see Fig. 5B).

Each of the three first steps in preparation methods C3a–c lasted for 10 min and the applied currents were 10 mA, 20 mA and 30 mA, respectively. In all three cases the resulting surfaces consisted of differently sized spherulites (2–15 μm), depending on

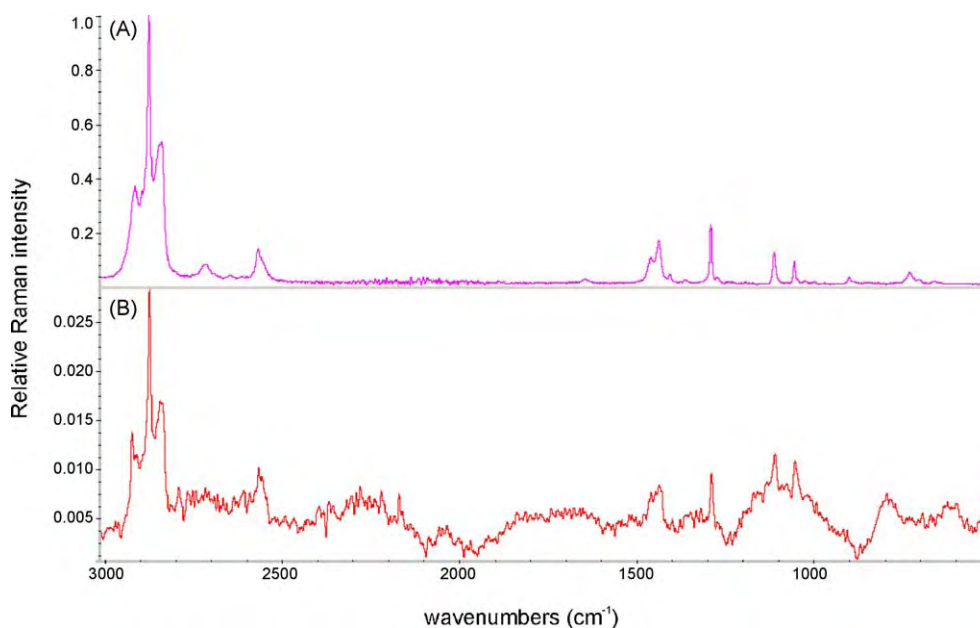


Fig. 6. Raw FT-Raman spectrum of pure 16-MHDA in the condensed state (A) and Raman spectrum of 16-MHDA adsorbed onto copper SERS-active substrate prepared from an acid bath (procedure A2b) (B).

the duration of the final step. The application of a 40 mA current for 15 min (method C3c) led to smaller spherulites (2–5 μm). When the 40 mA current was applied for 30 min (method C3b) the sphere-like features on the surface were larger (5–15 μm). SEM images of these structures are shown in Fig. 5C and D.

3.2. SERS spectra of deposited organics thiols

Organic thiols (16-MHDA and 4-ABT) were deposited onto all copper SERS-active substrates as described above and their Raman spectra were subsequently measured. The efficiency of surface enhancement was evaluated by comparing the Raman intensity and structure of characteristic bands in the obtained spectra. In order to determine the influence of surface morphology and surface roughness values on the enhancement factor of Raman signal on substrates prepared from an acidic bath, 16-MHDA spectra obtained from these substrates and FT-Raman spectrum of pure 16-MHDA in condensed state were compared. The Raman spectrum of 16-MHDA deposited on a substrate prepared by method A2b showed an extremely weak or negligible enhancement of Raman signal intensity (see Fig. 6). Due to poor signal-to-noise ratio, very few characteristic bands could be positively recognized in these spectra, which were therefore insufficient for the proper identification of the analyte. The presence of the compound on the surface can be distinguished due to characteristic bands of stretching vibration of CH_2 groups in the region 2840–2950 cm^{-1} . Other characteristic Raman spectral bands (CH_2 bending vibration at 1452 cm^{-1} , COC stretching vibrations at ca 1300 cm^{-1} and ca 1125 cm^{-1}) were in this spectrum of a much lower intensity and all spectral information was distorted by noise. In order to evaluate the ability of the substrates to enhance Raman signal of adsorbed model analytes, we compared the intensities of a Raman band assigned to COC stretching vibration of 16-MHDA at ca 1300 cm^{-1} in the series of spectra measured under similar experimental conditions on the various substrates examined. The change in Raman signal intensity between spectra corresponding to two substrates can be expressed as numerical value of Raman signal intensity ratio (RSIR). Spectra obtained from substrates A1a, A1b and A2a were very similar to the spectrum measured on the substrate A2b described above: only some of the characteristic

bands appeared and the intensity of Raman signal and the S/N ratio were also rather low. The values of RSIR were comparable, in the range of 1–1.5 (A1a/A2b, A1b/A2b and A2a/A2b). We can conclude that substrates prepared from the acidic baths are not suitable for SERS measurements due to low enhancement of Raman signal and high noise level. Different surface roughness values (described above) showed almost no influence on the degree of Raman enhancement.

A much better SERS enhancement was observed on substrates prepared from ammoniac baths. The effect of the conditions of electrochemical deposition procedure (the duration of individual current steps, current value difference between the steps, and the final current value, summarized in Fig. 2) on the surface morphology and SERS enhancement was systematically investigated. It was found that the surface enhancement of Raman signal was the highest when shorter individual current steps were applied. The final current value was found to be a crucial parameter for the formation of surface morphology.

In Fig. 7, the SERS spectra of 16-MHDA on C1b, C2b and C3b substrates are compared. Raman spectra obtained on substrates C1 showed very high intensity and a very good S/N ratio (noise on peaks is negligible; the noise oscillations on background curve are very weak). The RSIR value for substrates C1b/C3b and C2b/C3b is 10 and 5, respectively. All major characteristic Raman bands were apparent with good resolution and could be properly identified. The substrate surfaces were homogeneous and macroscopically uniform, thus these substrates are also suitable for further modification of a deposited organic layer and its subsequent Raman spectral mapping. The C1 substrates showed the best values of RSIR and high S/N ratio also in the case of 4-ABT SERS spectra (data not shown). As was mentioned above, the surface of this substrate was covered by cauliflower-like structures. The EM mechanism of SERS is based on the interaction of electric field of incident radiation with the nanostructure features of the metal surface and produces locally extremely large electric field intensities.

Aggregation of two or more nanostructured features into larger clusters can lead to the formation of “hot spots”, each of which possesses its own characteristics of polarization and field strength and where the extremely strong electric field is non-uniformly

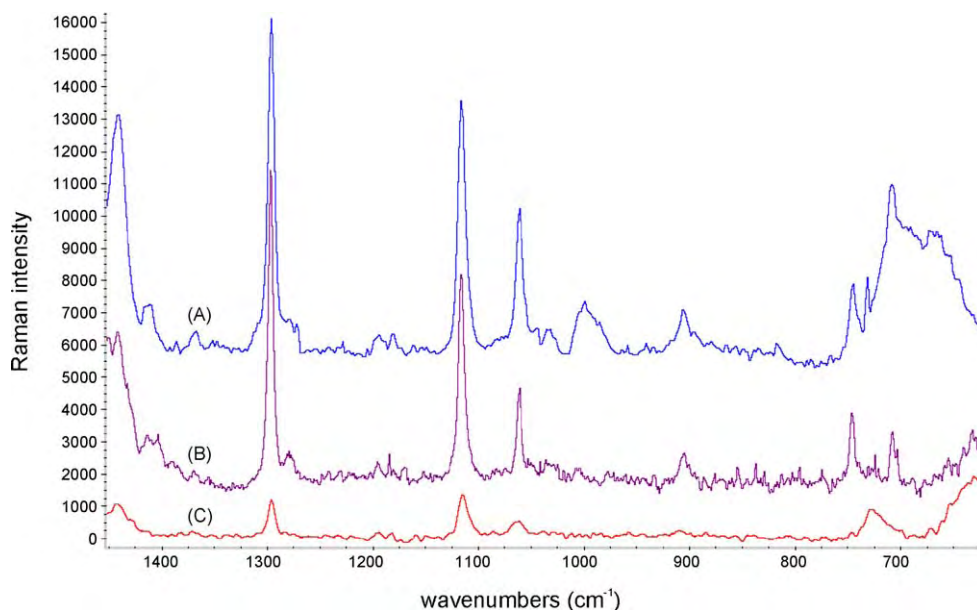


Fig. 7. Raw Raman spectra of 16-MHDA adsorbed onto copper SERS-active substrates prepared according to procedure C1b (A), C2b (B) and C3b (C).

distributed and spatially localized. From SEM images of cauliflower structures, it can be seen that the surface of this substrates consists of nanostructured features which best match the requirement for the formation of hot spots. Cauliflower surface consists of long spear-shaped structures covered by assemblies of smaller round-shaped particles. The clusters of these assembled copper spheres could include the hot spots which increase EM field in their close proximity and hence cause the enhancement of Raman signal of an adsorbed molecule.

In comparison to C1, Raman spectra from substrates C2 showed much lower intensity, low S/N ratio, lower RSIR ($C2/C1 = 0.5$) and the resolution of the structure of the main characteristic bands was less clear for further interpretation. Nevertheless, the main characteristic bands were present. The main difference in individual preparation procedures within the C2 group was the final current value, which was found to be a very important parameter in terms of surface enhancement factor. In the case of C2a procedure, where current value in the final step was the same as in the C1 group (70 mA), the subsequent Raman spectral measurements showed comparable spectral information with C1 substrates for both analytes in terms of both intensities (RSIR ca 1) and resolution of Raman bands. But on the substrates prepared according to further C2 procedures (C2x, where $x = b, c, d$) with lower current values in the final step, a progressive downgrade in the quality of the Raman spectra was apparent. Thus, it can be concluded that for the ammoniac baths and preparation procedures used in this work, high final current value is necessary to form surfaces with good enhancement of Raman signal of deposited compounds.

Finally, Raman spectra obtained from substrates C3 showed a low intensity of all Raman bands, although characteristic peaks were still visible. The spheroidal copper particles on the surface of these substrates were probably too large (several μm) to fulfill the condition of optimal surface plasmon resonance and to cause proper surface enhancement of the Raman signal. However, from SEM images of these substrates it was found that the size of the formed particles can be modified by the duration of the final step with a high current: the mean particle size was approximately 5 μm on C3b against approximately 10 μm on C3c (Fig. 5C and D). Hence, this procedure may have a potential for further optimization. From the point of view of the relation of Raman enhancement

with the surface morphology, we can assume that inter-particle distances of individual copper particles of C3 substrates are not suitable for their mutual dipole–dipole interaction and do not cause an increase in the magnitude of induced dipole and hence the polarization.

4. Conclusion

In the present work, copper SERS-active substrates prepared by electrochemical deposition were characterized by AFM and SEM. These methods provide complementary information about the arrangement and size of features on roughened metal surfaces. In the case of AFM, the surface roughness can be evaluated quantitatively, thus providing useful information in the elucidation of the SERS phenomenon. Copper SERS-active substrates were prepared in different ways with the aim of finding conditions for optimum SERS enhancement.

The results of Raman measurements showed that an acidic bath is not particularly suitable for the preparation of copper SERS-active substrates and for obtaining a good SERS enhancement. Measured Raman spectra showed a low S/N ratio and low intensities, moreover some characteristic bands were missing. Substrates prepared from ammoniac baths exhibited much better enhancement in all measured spectra of the selected probe molecules, but the parameters of the preparation procedure had to be optimized.

The application of short current steps results in the formation of irregular copper barb-like particles that exhibit a relatively low enhancement (C2c, C2d). The short time is probably not sufficient for the formation of more regular copper particles. Thus, the duration of individual steps is a crucial parameter for the formation of the nanoscale surface morphology. When current steps are prolonged, this results in the formation of regular spherical particles of different size (C3 procedures). It was found that the final current is also a critical parameter for surface morphology, because its value and the duration of the step affected the size of the particles (C3b vs. C3c).

It appears that when a current sequence of short steps ends with one long step with a high current value (C1 procedures), barb-like particles become coated with spherical particles (cauliflower-like surface morphology). Raman spectra obtained from these

substrates exhibit remarkably strong SERS enhancement, extremely high S/N ratio, high spectral intensities and all characteristic Raman bands required for proper spectral interpretation are present.

In conclusion, it has been shown that good Raman surface enhancement can be achieved on copper SERS-active substrates prepared by electrochemical deposition from ammoniac baths. Copper substrates fabricated from acidic baths did not show efficient Raman surface enhancement. It appears that the average surface roughness value does not play a substantial role, but the shape of nanostructures is a key parameter. Composite structures consisting of fractal spear-shaped structures with superimposed spherulite features were found to give the best SERS enhancement from all cases tested in this work.

Acknowledgements

This work has been supported by the Grant Agency of the Czech Republic (GD 104/08/H055), by Grant Agency of the Czech Academy of Science (KAN 208240651), by Ministry of Education, Youth and Sports of the Czech Republic (MSM 6046137307, MSM 604617306) and by Department of Research and Development of the Institute of Chemical Technology Prague (402080016).

References

- [1] S. Nie, S.R. Emory, *Science* 275 (1997) 1102.
- [2] E. Smith, G. Dent, *Modern Raman Spectroscopy: A Practical Approach*, John Wiley & Sons, Chichester, United Kingdom, 2005.
- [3] A. Otto, *Journal of Raman Spectroscopy* (2005) 497.
- [4] A. Kudelski, J. Bukowska, *Vibrational Spectroscopy* 10 (1996) 335.
- [5] R.P. Van Duyne, J.C. Hulteen, D.A. Treichel, *Journal of Chemical Physics* 99 (1993) 2101.
- [6] B. Bozzini, L. D'Urzo, M. Re, F. De Riccardis, *Journal of Applied Electrochemistry* 38 (2008) 1561.
- [7] C.G. Blatchford, J.R. Campbell, J.A. Creighton, *Surface Science* 120 (1982) 435.
- [8] N.A.A. Hatab, J.M. Oran, M.J. Sepaniak, *ACS Nano* 2 (2008) 377.
- [9] B.N.J. Persson, Z. Ke, Z. Zhenyu, *Physical Review Letters* 96 (2006) 207401.
- [10] K.S. Shin, H. Ryoo, Y.M. Lee, K. Kin, *Bulletin of the Korean Society* 29 (2008) 445.
- [11] S. Zou, M.J. Weaver, X.Q. Li, B. Ren, Z.Q. Tian, *Journal of Physical Chemistry B* 103 (1999) 4218.
- [12] Q.j. Huang, J.L. Yao, B.W. Mao, R.A. Gu, Z.Q. Tian, *Chemical Physics Letters* 271 (1997) 101.
- [13] B. Ren, G.K. Liu, X.B. Lian, Z.L. Yang, Z.Q. Tian, *Analytical and Bioanalytical Chemistry* 388 (2007) 29.
- [14] G. Binnig, C.F. Quate, C. Gerber, *Physical Review Letters* 56 (1986) 930.
- [15] V. Prokopec, J. Cejkova, P. Matejka, P. Hasal, *Surface and Interface Analysis* 40 (2008) 601.
- [16] M. Clupek, V. Prokopec, P. Matejka, K. Volka, *Journal of Raman Spectroscopy* 39 (2008) 515.
- [17] K.S. Shin, H.S. Lee, S.W. Joo, K. Kim, *Journal of Physical Chemistry C* 111 (2007) 15223.
- [18] K. Kim, H.S. Lee, *Journal of Physical Chemistry B* 109 (2005) 18929.
- [19] B. Bozzini, L. D'Urzo, C. Mele, V. Romanello, *Journal of Materials Science—Materials in Electronics* 17 (2006) 915.